28

Pneumatic Actuators for Climbing, Walking and Serpentine Robots[1]

Grzegorz Granosik
Technical University of Lodz
Poland

1. Introduction

This chapter presents construction, control, advantages and disadvantages of various pneumatic actuators we have been using in several projects of climbing, walking and serpentine robots during last 13 years. We start with qualitative and quantitative analysis of different actuators. This part is mostly based on the literature review but augmented with our own experience related to these particular types of robots. We focus on pneumatic drives as very suitable for robots having permanent contact with unknown environment. Then we show a few constructions developed in our laboratory: starting from light weight manipulator for climbing robot, quadruped walker and climber, jumping and worm-like robots, see Fig. 1. We also present our contribution in development of the family of serpentine robots designed at the University of Michigan (UofM).

There are some general requirements for joint actuators in mobile robots designed for regular contact with ground (obstacles). Listed here are the six most important ones:

1. Joint actuators should be capable of developing sufficient force to lift whole robot or its parts in order to climb or overcome obstacles, or to operate with load.
2. Joint angles should be controllable proportionally.
3. Another key requirement is that mobile robots should conform to the terrain compliantly. This assures correct propulsion and safe manipulation as well as dynamic isolation of main body (controller) from ground. Robots that don't conform compliantly require complex sensor systems to measure contact forces and to command a momentary angle for each non-compliant joint accordingly.
4. At times it is necessary to increase the stiffness of a joint, for example to cross a gap or precisely track position trajectory. Alternatively, it may be necessary to adjust the stiffness to an intermediate level, for example to change jumping frequency. Thus, considered mobile robots and manipulators must be capable of adjusting the stiffness of every DOF individually and proportionally.
5. Joint actuators should be scalable to fit robots of different sizes. It is convenient to use the same technology in mini- and macro-scale.

[1] This research was partially financed by the Ministry of Science and Higher Education under grant No 3 T11A 023 30 and 3 T11A 024 30

Source: Bioinspiration and Robotics: Walking and Climbing Robots, Book edited by: Maki K. Habib
ISBN 978-3-902613-15-8, pp. 544, I-Tech, Vienna, Austria, EU, September 2007

6. The energy consumption and weight of the actuators should be minimal, because energy is a limited resource in an untethered mobile robot.

Figure 1. We contributed in these robots: (from top left) TM44 manipulator for climbing robot Robug III, Spike Junior – climbing robot, jumping leg, bellows driven crawler, OmniTread - serpentine robot developed at UofM

2. Review of Candidate Joint Actuators

There are many different ways of actuating joints in a mechanical structure. However, only a few of them can provide the range of motion and force required for actuating legs of walkers and climbers or joints of a serpentine robot. Those actuators are electrical motors, hydraulic motors or actuators, and pneumatic actuators. Table 1 lists some key parameters for candidate joint actuators.

2.1 Actuation Stress/Strain analysis

In order to find the best-suited actuators for various robots we performed a detailed analysis mostly based on the comparison of performance indices of mechanical actuators introduced by Huber et al. (1997) and complemented by our own investigations (Granosik & Borenstein, 2005; Jezierski, 2006). The original paper did not include electric motors. It also included only select types of pneumatic actuators. We calculated the performance indices for a few pneumatic bellows and artificial pneumatic muscles.

Huber et al. introduced the measures of *actuation stress*, σ, and *actuation strain*, ε. Actuation stress represents a measure of force divided by the active area of the actuator:

$$\sigma = \frac{F_{\max}}{A_{act}} \tag{1}$$

where F_{max} is the maximal force the actuator can provide and A_{act} is the active area of the actuator. For example, in a pneumatic actuator the active area is the area of the piston.

Actuation strain represents a measure of how much an actuator can extend in relation to its fully retracted state:

$$\varepsilon = \frac{L_{\max} - L_{\min}}{L_{\min}} \tag{2}$$

where L_{max} and L_{min} are the length of the actuator at maximal and minimal extension, respectively.

In most cylinder-type actuators actuation strain is limited to 1.0, because the piston and rod cannot move through a greater distance than one cylinder length. In pneumatic bellows the actuation strain can reach 4. Huber et al. constructed a graph that plots actuation stress versus actuation strain. We reproduced this graph, with some modifications (explained below), in Fig. 2.

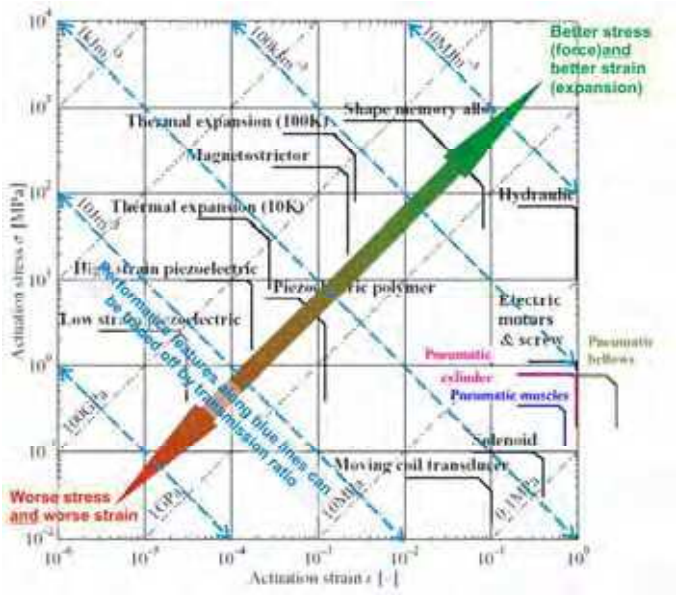

Figure 2. Actuation stress versus actuation strain for various actuators - reproduced from Huber et al. (1997) and augmented with own data

The original paper of Huber et al. did not include electric motors. It also included only select types of pneumatic actuators. We were interested in including electric motors in the selection process, even though the performance of naturally rotary actuators cannot be formally expressed in terms of actuation stress and strain. Nonetheless, we made some reasonable assumptions about the transformation of rotary motion to linear motion and computed rough values for what we call "*equivalent actuation stress*" and "*equivalent actuation strain*" of electric motors this way. Specifically, we calculated the performance indices for some electric motors with a ball screw transmission mechanism that produces reasonable linear speed and force. To calculate the *equivalent actuation stress* we used the cross section area of the motor including the ball screw mechanism. We also calculated the performance indices for a few pneumatic bellows and so-called McKibben muscles (see Section 3) and added those results in Fig. 2.

Huber's graph in Fig. 2 can help designers identify suitable actuators for their application. For example, lines of slope -1 group actuators with approximately the same *volumetric stroke*

work. Huber et al. defined "*volumetric stroke work*" as the physical work (force × distance) available from one stroke movement per unit volume of the actuator. This means that pneumatic actuators can produce four orders of magnitude more work per unit volume than piezoelectric actuators. Since the physical work is approximately the same along lines of slope -1, the relations between stress and strain can be traded off by transmission mechanisms. Lines of slope +1 group actuators with similar stiffness, i.e., with similar ratios of σ/ε. Also, the thick lines in Fig. 2 indicate the upper performance limits of different actuators. Those actuators that are closest to the top right corner of Fig. 2 are naturally suited to lifting weights and propelling masses in the orders of magnitude required for mobile robots. Actuators closest to the lower left corner, such as piezoactuators, are better suited for micro-actuation (as presented, for example, by Magnussen et al., 1995 or Sun et al., 2001).

For walking and serpentine robots, one should limit the pool of candidate actuators to those plotted near the right side of Fig. 2, since actuators plotted there provide enough motion for the actuation of the robot's joints. However, in the case of mobile robots not only do actuation stress and strain have to be optimal, but also the actuator's weight has to be minimal. This means that we have to analyze what Huber et al. called "*specific actuation stress*." The resulting graph of specific actuation stress vs. strain reproduced from Huber et al. (1997) and augmented with our indices for pneumatic muscle, pneumatic bellows, and electric motors is shown in Fig. 3.

Figure 3 is similar to Fig. 2, but here the y-axis shows actuation stress divided by actuator density, or "*specific actuation stress*." As in Fig. 2, we added lines representing pneumatic bellows and electric motors, making the same assumption as explained earlier. As is apparent from Fig. 3, the superior characteristics of hydraulics (compared to pneumatics) are diminished once actuation stress is related to actuator density. Furthermore, hydraulics also becomes less desirable over electric motors once efficiency is considered, as was shown in Table 1.

Drive type \performance compared	Electric	Hydraulic	Pneumatic
Efficiency* [%]	(<1) 50-55 (>90)	30-35	15-25
Power to weight ratio [W/kg]	25-150	650	300
Force to cross section area [N/cm^2]	0.3-1.5	2000	100
Durability [cycles]	5-9·10^5	6·10^6	>10^7
Stiffness [kN/mm]	10-120	30	1
Overload ratio [%]	25	50	50-150
Linear movements ranges [m]	0.3 – 5	0.02 – 2	0.05 – 3
Linear velocity [m/s]	0.001 – 5	0.002 – 2	0.05 – 30
Positioning precision [mm]	0.005	0.1 – 0.05	0.1
Reliability (relative)	Normal	Worse	Better
Maintenance costs (relative)	Normal	Higher	Lower
Unfavorable features	Electric hazard, magnetic disturbances, heating	Leakages, difficult energy transmission	Noisy
Favorable features	Easy energy transmission and storage		Safety

Table 1. Key parameters of different actuators (based on Olszewski, 1998; Jezierski, 2006)
* The efficiency value in this table already includes a "penalty" for producing pneumatic or hydraulic pressure from a rotary source of mechanical power. Some of electric actuators using temperature to generate force have very low efficiency while piezoelectric phenomena give very high effectiveness; the medium values are for the most popular electric actuators – motors with reduction gears

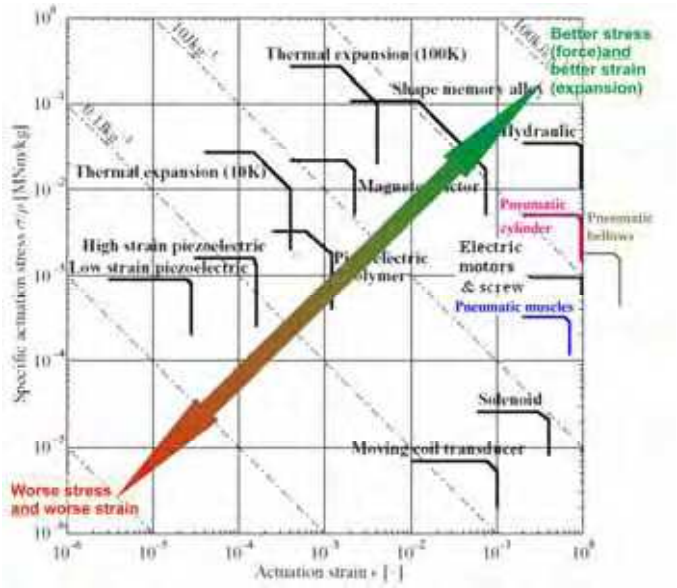

Figure 3. Specific actuation stress versus actuation strain for various actuators – reproduced from Huber et al. (1997) and augmented with own data

One should also note that Figure 3 considers the actuator only, but without the weight of the compressor or pump, and without the weight of manifolds, valves, fittings, and pipes. It is difficult to calculate the specific actuation stress for the whole actuation system with precision because the weight strongly depends on the application. However, both the lines representing hydraulic and pneumatic actuators have to be shifted down when the entire actuation system is considered. This is one of the reasons why electric actuation is usually chosen for freely moving robots while hydraulic or pneumatic actuation is mostly reserved for tethered robots. Another advantage of electric motors – not reflected in either Fig. 2 or Fig. 3 – is that electric motors are considerably easier to control and less expensive in most cases. Furthermore, energy is typically stored in electric form, which makes electric motors a preferable choice. Once these considerations are taken into account, in addition to the actuation stress/strain analysis illustrated by Fig. 2 and Fig. 3, it appears evident that there is some advantage to electric motors.

2.2 Natural Compliance

The actuation stress/strain analysis and discussion in the proceeding section showed some apparent advantage for electric motors, with respect to the actuation of joints in mobile robots and manipulators. However, there is another consideration, which, in our opinion, is of primary importance: natural compliance. We believe that natural compliance is critical for robots, whose propulsion depends on optimal traction between its propulsion elements (i.e., legs, wheels, or treads) and arbitrarily shaped environments, such as the rubble of a collapsed building or the rugged floor of a cave. It is also important for safe cooperation between robots or human and robot when unexpected contact can appear.

As mentioned in the proceeding section, the lines of slope +1 in Fig. 2 are related to the stiffness of the actuators. Hydraulic systems provide several orders of magnitude greater stiffness than pneumatic systems, which, in turn, are stiffer then electric motors without closed loop position control. But electric motors do require closed-loop control and have to be considered in this configuration. That means that the working stiffness of electric motors depends on parameters of the control loop. However, this is true for the motors only; if gearboxes or transmissions are added, then elasticity is eliminated. This makes electric drives ideal for accurate position control, but not for compliance.

Figure 4. Series elastic actuator with electric motor (reproduced from Robinson, 2000)

Robinson (2000) offered a work-around for this inherent limitation. He demonstrated that elasticity could be added to an inherently stiff actuator to allow accurate force and position-force control. He accomplished this by adding a soft spring in series with an electric motor with ball screw transmission or to a hydraulic cylinder (see Fig. 4). Special control algorithms allowed his system to produce a controllable force. He demon-strated application of this compliant actuator for dynamically walking biped. However, this approach substantially reduces the actuation strain and increases the weight of the actuator, which is then no longer suitable for serpentine robots or climbing machines.

We therefore conclude that pneumatic actuators are the only devices that provide *natural compliance*. The price we pay for natural compliance is the need for an onboard air compressor as well as the lower energy efficiency of the pneumatic system. We have ruled out the use of onboard liquid carbon dioxide tanks instead of an onboard compressor because of limitations in the amount of fluid they can carry.

The pneumatic actuator family is located in-between hydraulics and electric actuators in Fig. 3 and very close to electric actuators in Fig. 2. In practice pneumatic actuators behave as natural air springs, and, when used in closed-loop systems, can work as position-force actuators. Moreover, changes in working pressure can control the stiffness of pneumatic actuators from very limp (compliant) to very stiff. It is this fundamentally important property that makes pneumatic actuation the preferred choice for many mobile robots.

3. Pneumatic actuators

A variety of pneumatic actuators warrant consideration as possible joint actuators for walking, climbing and serpentine mobile robots. They are also recalled in reviews regarding driving mechanisms (Fukuda et al., 1999). In this section we compare some of these

actuators, including cylinders, muscles (McKibben and pleated), and bellows (off-the-shelf and custom-made). We will also present some uncommon types of pneumatic actuators. There are, in general, three types of pneumatic actuators: cylinders, muscles, and bellows. Cylinders and bellows develop force in quadratic proportion to their diameter *d*. In pneumatic muscles force is related to diameter and length, and the actuation force can be much larger than the force generated by a cylinder with the same diameter. However, a larger force requires greater length of the muscle, and the force drops very quickly with contraction. The actuation force of bellows also drops with expansion, but not nearly as dramatically as that of McKibben muscles. Because of their inherent geometric characteristics, cylinders and McKibben muscles have to be placed within a segment to actuate the joints and therefore are well suited to drive mobile manipulators and limbs of walking robots. On the other hand bellows are preferred for serpentine robots (we addressed this in details in our paper Granosik & Borenstein, 2005). Properties of pneumatic actuators are discussed in this section.

3.1 Pneumatic Cylinders

Cylinder-type actuators are by far the most popular ones. They are characterized by a stiff (usually aluminium) frame and a sealed piston, which slides inside. Depending on their construction, cylinder-type actuators can produce linear movements in one or both directions. The external shape of the cylinder is constant during all working cycles, except, of course, for the moving rod. The inherent disadvantage of cylinders is the friction caused by the necessarily airtight seal between the piston and the internal walls of the cylinder. This friction varies with pressure. The actuation strain of cylinder-type actuators is always less then 1. Pneumatic cylinders originally limited to on/off operation now become more and more popular (Bobrow & McDonell, 1998; Mattiazzo et al., 2002). We also present a few our own robotic applications of pneumatic cylinders in the further sections.

3.2 Pneumatic Muscles

Pneumatic muscles, similar to natural muscles, are typically one-directional actuators with pulling action. That means that for driving a single degree of freedom (DOF) two muscles are required. Pneumatic muscles are made from an elastic bladder reinforced externally or internally. One inherent disadvantage is hysteresis that is caused by the rubber bladder. Detailed analysis of construction and dynamics of pneumatic muscles can by found in Glenn et al. (2000) and Tsagarakis & Caldwell (2000). The first pneumatic muscle using an external reinforcing mesh is known as the *McKibben Artificial muscle.* McKibben muscles are fairy easy to manufacture in house (see Fig. 5a). They can be found in a variety of diameters and lengths and are commercially available for instance from the Shadow Robot Company (UK). The presence of two layers (bladder and mesh) can cause some friction and some problems with the construction. McKibben muscles usually need tendons to attach them to the links they actuate.

Some of these construction problems were resolved in the *Fluidic Muscles (MAS)* that are commercially available from Festo (Germany). Fluidic muscles have the reinforcement mesh integrated with the bladder and attached to standardized fittings (see Fig. 5b). However, these muscles are heavier than others because they are marketed as "industrial strength" devices. MAS muscles have been used by Berns et al. (2001) in an insect-like walking robot. Actuation of both McKibben and Fluidic muscles is based on the braided structure of the

reinforcement, which, when pressurized, extends in diameter and shortens in length, thereby producing a tensile force. The non-linear relation between tension and contraction of Fluidic Muscle for different pressures is shown in Fig. 5c. Since the entire hull of the muscle generates the active force, that force can be 10 times larger than that generated by a cylinder with the same diameter as the Fluidic Muscle in its initial state.
Another type of reinforcement is used in the so-called *Pleated Pneumatic Artificial Muscles* (PPAM). The PPAM was first introduced by Verelst et al. (2000). The PPAM was also presented by Morecki (2001) and applied in robot actuation by Van Ham et al. (2002). The reinforcing strings are arranged in parallel along the muscle and are moulded inside the rubber bladder (see Fig. 5d). They can produce even larger forces than Fluidic Muscles, as shown in Fig. 5e. However, this type of muscle increases its diameter more then tree times when maximally contracted.

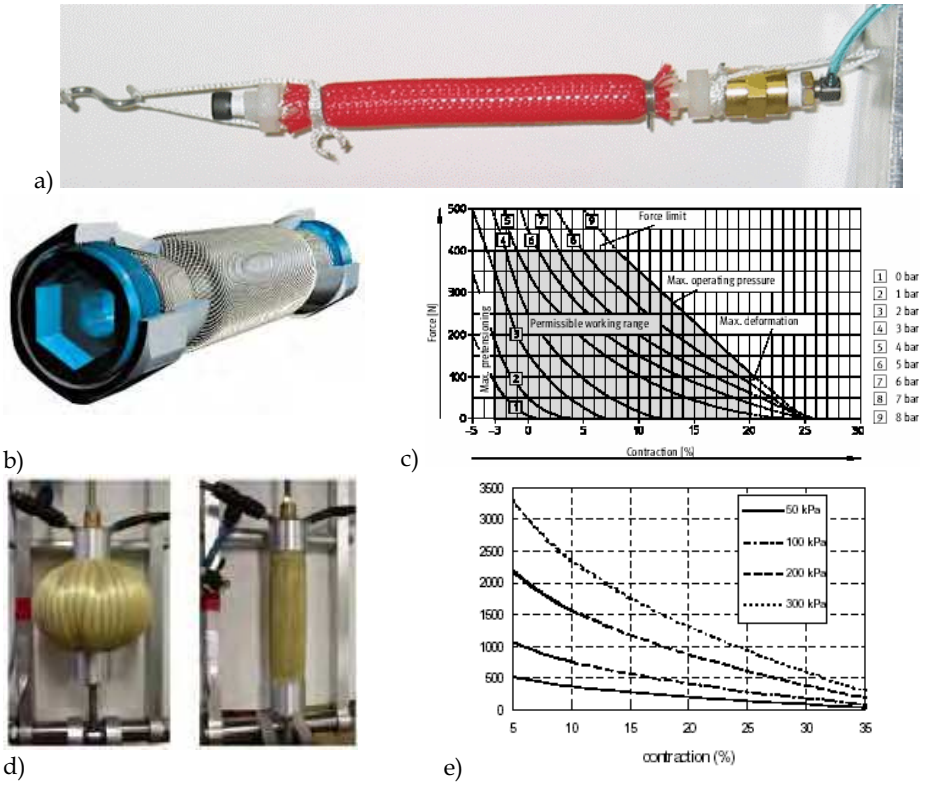

Figure 5. Pneumatic muscles: a) McKibben type (house made), b) MAS Fluidic Muscles (Festo), c) Relation between tension and contraction for different pressures (reproduced from Festo catalogue), d) Pleated Pneumatic Artificial Muscles (PPAM) – reproduced from Verelst et al. (2000), e) Relation between tension and contraction of PPAM for different pressures (reproduced from Verelst et al., 2000)

In summary, pneumatic muscles are flexible actuators, which, when pressurized, increase in diameter and contract because of their diagonal-mesh reinforcements. They can produce large forces but for small contractions only and the value of tension decreases with

increasing contraction. The useful actuation strain is between 5-30% of the initial length. Pneumatic muscles are elastic and therefore can conform easily to skeleton of manipulator or walking robot, they can also drive joints having more than one degree of freedom (DOF) – so called multi DOF – usually found in the kinematic structure of biologically inspired robots (Feja, 2006).

3.3 Pneumatic Bellows

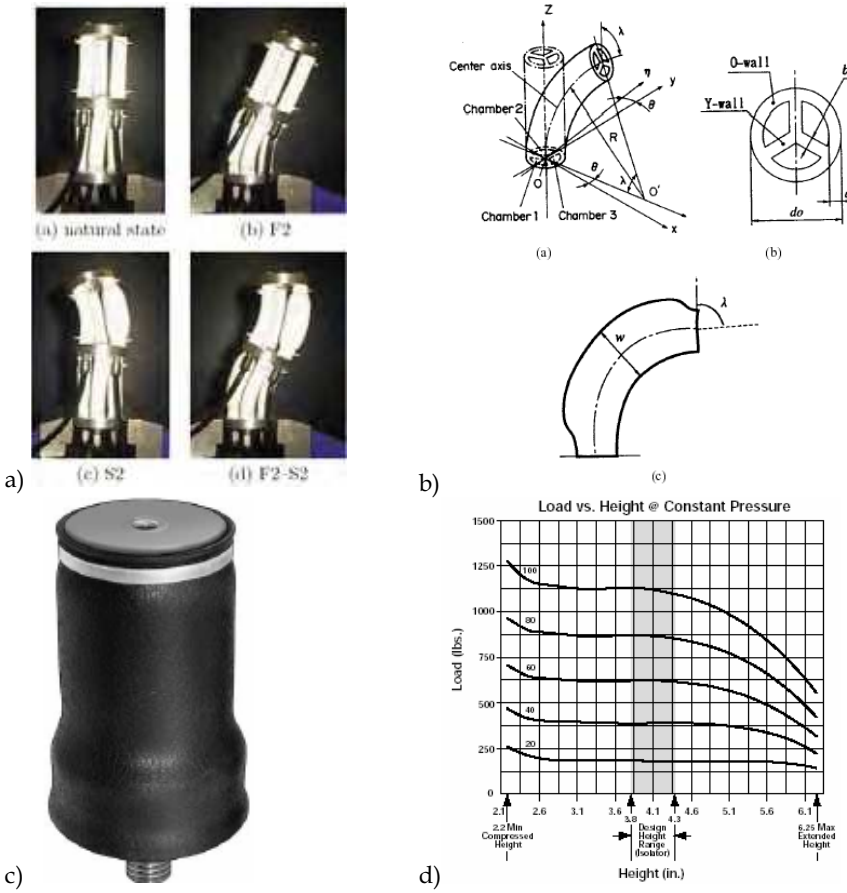

Figure 6. Pneumatic bellows: a) pneumatic group actuator (reproduced from Hirai et al., 2002), b) flexible pneumatic microactuator (reproduced from Suzomori et al., 1997), c) thin-sleeve rubber bellows (reproduced from McMaster-Carr catalogue), d) static characteristics of thin sleeve bellow (reproduced from McMaster-Carr)

The third type of pneumatic actuators is the bellows. Bellows are elastic structures performing one-directional (pushing) action. They are either made out of a very thick-walled rubber tube or they require external reinforcement to appropriately direct force in longitudinal direction. This type of actuation is used only rarely for robotic actuation. Shimizu et al. (1995) proposed a hexahedron actuator to drive rotational joints and Hirai et

al. (2002) presented a pneumatic group actuator for trunk-like robot (see Fig. 6a). Schultz et al. (2001) also address the bellow-type of actuation as based on insect's constitution. A variation of a group actuator is the flexible pneumatic microactuator introduced by Suzomori et al. (1997), shown in Fig. 6b. The latter is an example for the possible downward scalability of bellow-type actuators. Yet another type of bellows was used by Aoki et al. (2002) in joints of Slim Slime Robot. These are steel bellows covering whole joint of robot, internally driven by compressed air and steered by three motorized bridles.

Unlike in robotics, pneumatic bellows (or rubber air-springs, which have a slightly different shape) are widely used in car or truck suspension systems (see Fig. 6c). Air springs are usually used in a very small range of motion even though they can produce actuation strain of about 300% of their initial length, as shown in Fig. 6d. This feature is a great advantage when compared to other actuators.

The force generated by bellows is proportional to the applied pressure and cross section area. In this sense bellows actuator acts similarly to cylinders. However, since bellows' side walls are made of rubber their diameter expands when inflated. Bellows have usually bulky fittings on both ends and are made of relatively thick rubber, which makes them heavier than similar-sized cylinders. To overcome this disadvantage we developed the alternative pneumatic bellows shown in Fig. 7. It consists of a neoprene-coated nylon shell, reinforced with metal rings and bonded to metal plates with fittings on both ends. The external diameter is nominally 4.4 cm and it expands to only 4.6 cm when inflated. Our bellows changes length from 2.5 cm to 10 cm (i.e., it has an actuation strain of 4) and it works with pressures up to 0.7 MPa (100 psi).

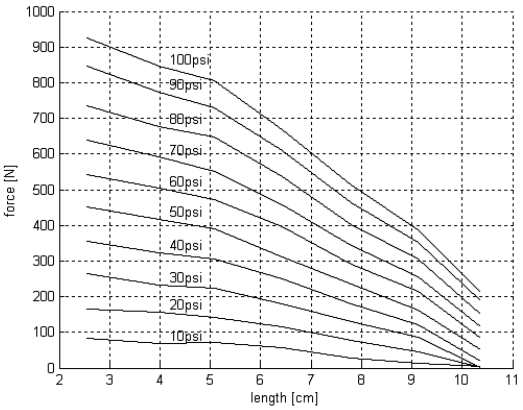

Figure 7. Rubber bellows developed in Mobile Robotics Lab (UofM) - used in the OmniTread. Static characteristic of bellows (right)

We have shown feasibility of all kinds of pneumatic actuators for joint actuation of various mobile robots and manipulators. Comparison led to the conclusions that pneumatic cylinders and muscles are more suited for manipulators and limbs of walking and climbing robots, while bellows are best suited for the actuation of articulated joints in serpentine mobile robots. In further sections we will show a few case studies of pneumatically driven robots.

4. Position and force control of pneumatic drives

Many different methods of a position control of a pneumatic cylinder are presented in the literature (Janiszowski & Olszewski,1994; Tang & Walker, 1995; Kadowaki 1996; Drakunov et al., 1997; Kurek & Prończuk, 1997; Olszewski 1998; Shih & Ma, 1998; Sorli & Vigliani, 1998; Bobrow & McDonell, 1999). However, most of them describe stand alone actuator with specialised position control algorithm. In contrary for robotic applications it is more natural to employ standard position or/and force control schemes and adjust pneumatic drives for such a task (Bobrow & McDonell, 1999; Granosik 2001b). We present this concept for a pneumatic drive consisting of pressure proportional valve, long pipe and double acting cylinder. Identification of the plant in a frequency domain is performed followed by pressure control loop synthesis and experimental verification. Finally pneumatic drive has been employed to a 2 DOF manipulator originally designed and built for walking robot (Collie et al., 1996).

4.1. Problem formulation

In the robotic applications the hierarchical control system is usually considered. The highest level providing position or/and force tracking and lower - torque control. When the pneumatic actuator is applied, driving torque in a manipulator joint has the form:

$$\begin{aligned} \tau(\theta,t) &= F(t)\cdot r(\theta) \\ f(t) &= A_1 p_1(t) - A_2 p_2(t) \end{aligned} \tag{3}$$

where: $\tau(\theta,t)$ – driving torque,

$F(t)$ – force generated by pneumatic double acting cylinder,

$r(\theta)$ – function of a joint position θ (depends on kinematics of transmission mechanism),

p_1, p_2, A_1, A_2 - pressures in the chambers of cylinder and cross sectional area of both sides of piston, respectively. Subscript *1* indicates rodless chamber.

Based on equations (3) the lowest level of pressure control for both sides of pneumatic cylinder can be assumed. We consider the set of pressure proportional pneumatic valve, pipe and chamber of cylinder. The schematic representation of pneumatic circuit is shown in Fig. 8. It should be noticed, that pressure sensor is mounted in the valve and doesn't measure exact pressure in a chamber, and moreover its signal is disturbed by large flow of the air in a valve. Problem of estimation of the pressure in cylinder is not trivial and is analysed in details in. Proposed pneumatic system was a result of two fundamental assumptions:

- reduction of the weight of the manipulator by moving all heavy components, like valves, down to the base,
- employing direct drive methods gives the simplicity and stiffness of transmission mechanisms.

The influence of valve flow-rate and length, and diameter of pipe was theoretically analysed, simulated and verified in (Sorli & Vigliani, 1998).

Another method based on identification of a whole system is proposed here. Number of experiments was performed leading to the set of Bode plots for different configurations of pipes and chamber volumes. The example plots are shown in Fig. 9 and Fig. 10. The experiments have been made for different lengths of pipe. The change in plots seems to be

obvious. The second order linear model described by equation (4) has been assumed for identification.

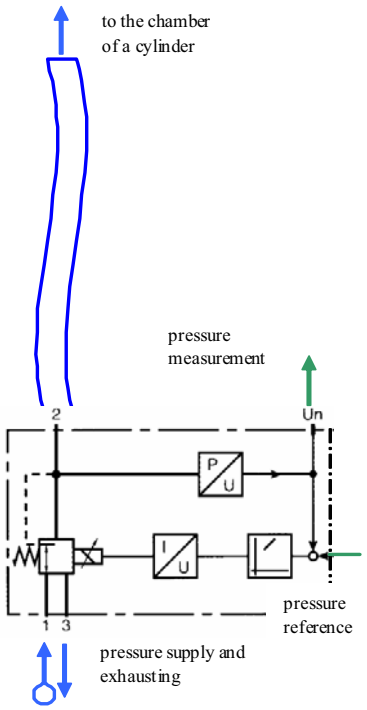

Figure 8. Pneumatic circuit

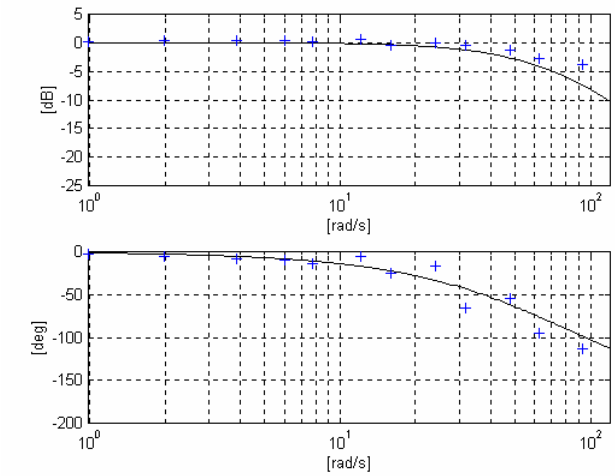

Figure 9. Bode plots of a pneumatic drive: proportional valve mounted directly to the cylinder and volume of a chamber 41cm^3

$$\ddot{y} + 2\xi\omega_n\dot{y} + \omega_n^2 y = \omega_n^2 u \tag{4}$$

where: u, y – input and output of a system, respectively,
ξ – damping coefficient,
ω_n – natural frequency of a system.

Coefficients of the model (4) depend on a pipe length and a chamber volume and are collected for different combinations of the components in a Table 2. Parameter x indicates a position of a piston measured from a rodless end of cylinder.

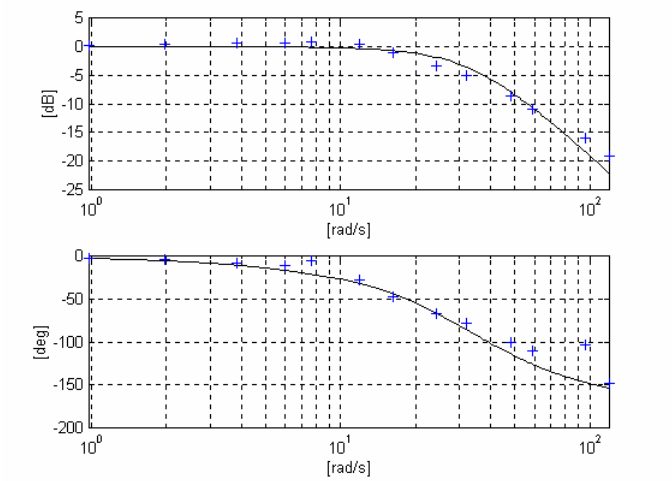

Figure 10. Bode plots of a pneumatic drive: proportional valve, pipe length 10cm, diameter ϕ= 4mm, and volume of a chamber 236cm³

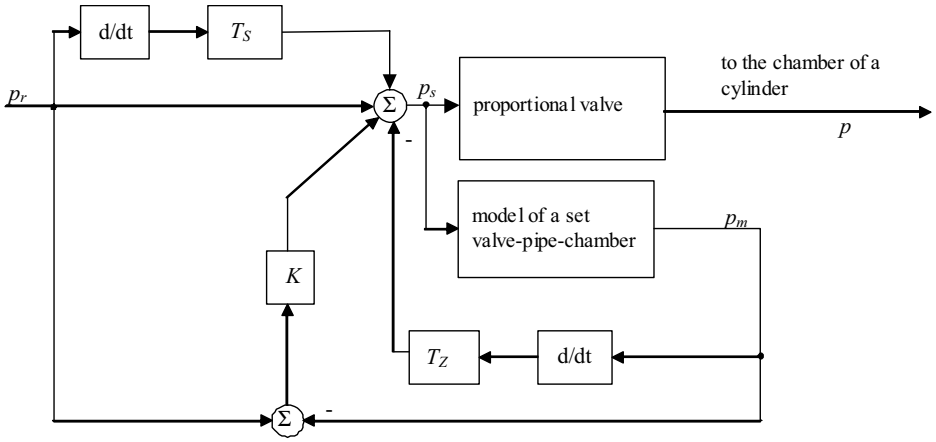

Figure 11. Scheme of a pressure control system

The further analysis and empirical verification have been made on a stand consisting of Sentronic valve (ASCO-Joucomatic), pipe of length 240cm and diameter ϕ4mm, and cylinder UDR 32-5 (Clippard).

Parameters of the plant	ξ	ω_h [rad/s]
valve mounted to the cylinder, chamber 1, x=12.7cm	0.8	34
valve mounted to the cylinder, chamber 1, x=2cm	1.0	80
pipe diameter ϕ6mm, length=40cm, chamber 1, x=12.7cm	1.0	25
pipe diameter ϕ4mm, length=240cm, chamber 1, x=12.7cm	1.0	8

Table 2. Coefficients of the model (4)

For a found model the pressure regulator is proposed with two loops for amplitude and phase correction as presented in Fig. 11. Model of a valve-pipe-chamber was employed for calculation of an unmeasured pressure in a chamber. An alternative solution can be proposed based on filtration of pressure signal gathered in a proportional valve.
The regulator settings T_z, K, T_s and plant parameters ξ, ω_h were calculated for a few piston positions and then approximated by quadratic polynomial. We obtained four functions $K(x)$, $T_S(x)$, $T_Z(x)$, $\omega_h(x)$, of piston position for both chambers of pneumatic cylinder (Granosik, 2001).

4.2. Experiments with position control

After testing valve-pipe-chamber model and pressure control algorithm in a quasi static mode we performed position trajectory tracking for 2 DOF manipulator. The external position feedback and classical computed torque algorithm have been employed. Tracking of the 5th order polynomial position trajectory of the 2 DOF manipulator is presented in Fig. 12. Plots obtained in the experiment are quite smooth and position error – presented in Fig. 13 – of 4 degrees is comparable with other applications presented in the literature (Bobrow & McDonell, 1999).

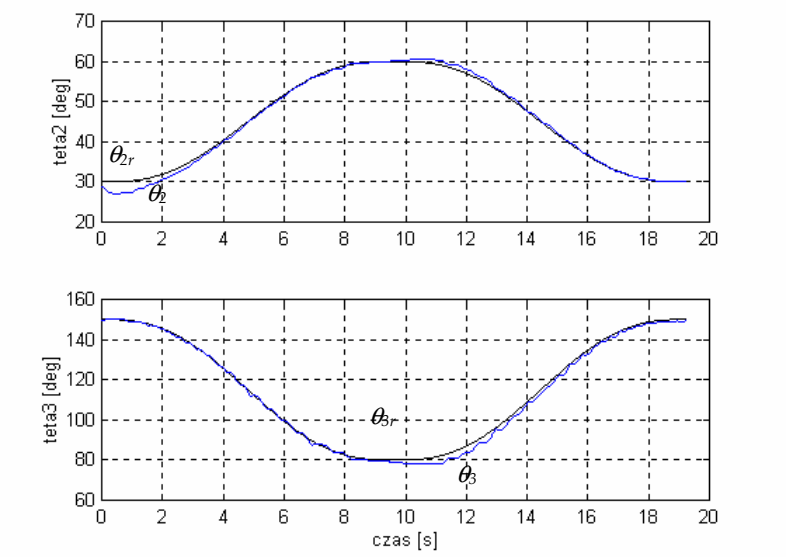

Figure 12. Position trajectory of 2 DOF manipulator, θ_2, θ_3 – position of first and second joint, respectively. Subscript r indicate reference trajectory

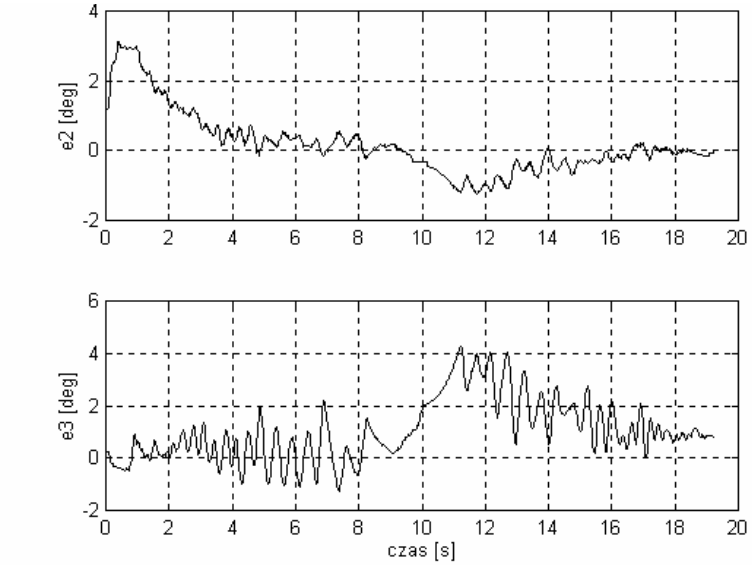

Figure 13. Plots of position errors in an experiment presented in Fig. 12

4.3. The spring model of the pneumatic drive

Each joint of manipulator or robot's leg driven by a pneumatic actuator can be seen as two-spring system shown schematically in Fig. 14. These springs represent features of compressed air in both chambers of the cylinder. There are five parameters that characterise the drive in this model: the initial lengths of springs l_1 and l_2, their compressibility constants k_1 and k_2, and the friction coefficient c. All these values are functions of volume and pressure of air in chambers that are regulated by a control system.

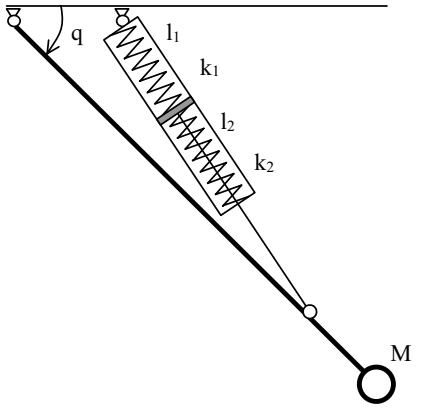

Figure 14. Spring representation of a pneumatic actuator

The dynamic model of such a system is rather complicated; even in the case when both chambers are closed (the controller does not act). The main reason of this is a non-linear kinematics of the system and a specific nature of friction between a piston and the cylinder.

However, the system should behave similar to a second order inertial object. To verify this hypothesis a following experiment was performed for one joint of the leg. After closing all valves supplying both chambers at a certain static position q_o (about 115^0) an external force F_e was applied to the leg to change the position of the join by q_m. Then the force was released and the position of the join versus time was collected. The results of four tests, for various levels of pressures, are shown in Fig. 15.
As it can be seen, the free oscillations of the leg are quite similar to the case of the second order system, where the position is described by the function (5):

$$q(t) = q_m e^{-\mu t} \cos(\omega t) + q_o \tag{5}$$

Using an identification procedure it is possible to find the best estimation of dumping coefficient μ and the angular frequency ω. The dumping coefficient changes in a quite wide range (from 0.54 for the lowest level of pressure up to 1.35 for the highest level), while the changes of the angular frequency are not so big (from 6 rad/s to 13 rad/s).
The experiment confirms that features of the drive depend significantly on the pressure level in both chambers of the actuator. There are two effects while the pressure level in the actuator is being increased. The first one consists in nearly proportional relationship between the pressure and the coefficient k in a spring model of the drive, what is described by the following relationship (6).

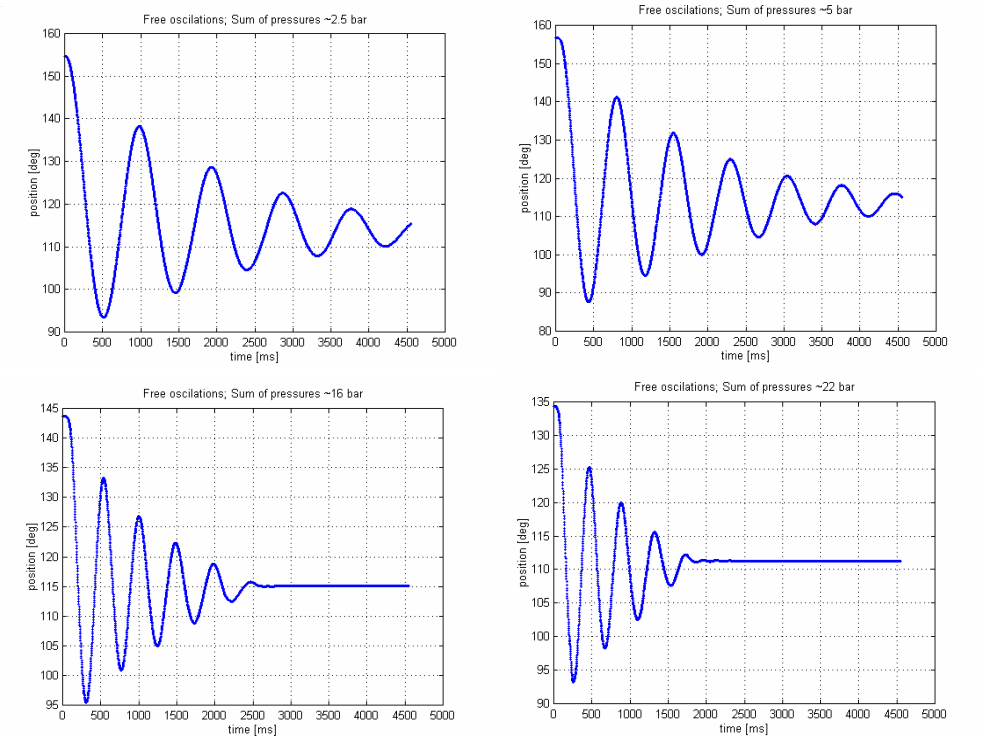

Figure 15. Free oscillations of a leg for different sums of pressures

$$\Delta f \cong A\left(\frac{p_{10}}{l_{10}}+\frac{p_{20}}{l_{20}}\right)\Delta l = k\Delta l \tag{6}$$

where p_{io} is the initial pressure in the i-th chamber, l_{io} is the initial length of this chamber, A denotes the cross-section area of the cylinder, and Δl is a displacement of the piston from its initial position.

The second effect of increasing the pressure level is a rise of the actuator's friction. An example dependency of static and dynamic friction versus sum of pressures for the applied actuator is shown in Fig. 16. This explains the relationship between the pressure level and the dumping coefficient μ in a spring model.

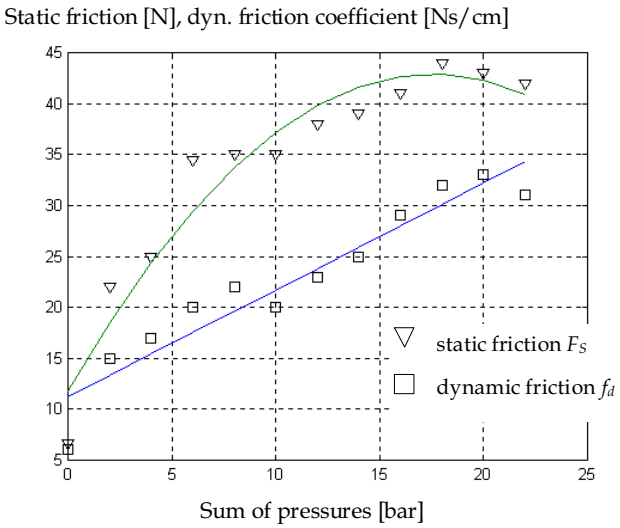

Figure 16. Static and dynamic friction forces versus sum of pressures in chambers

This analysis and experiments with pneumatically driven manipulator led us to the maximum stiffness rule for position control (Granosik & Jezierski, 1999) and further to position-force control (Granosik, 2001b). We also tested the influence of stiffness of drives on the contact forces rising when manipulator unexpectedly meets an obstacle.

4.4. Experiments with position-force control

Based on our experience with position control of TM44 manipulator we naturally used computed torque algorithm for position-force control. As we cannot define exact scenario of manipulator's task it is difficult to use hybrid control. On the other hand, impedance control does not close position and force feedback simultaneously. Combining these two algorithms and using Chiaverini & Sciavicco (1993) approach we proposed simultaneous position and force control with force feedback from JR3 sensor. Control system realizes Cartesian trajectory and monitors contact force. When contact appears, the system takes force feedback into account realizing prescribed trajectory (i.e. limiting contact force). In our TM44 manipulator we used an advantage of pneumatic drives – we implemented variable

stiffness control as shown in Fig. 17 where **M**, **C**, **G** are matrices from model of dynamics and $\mathbf{K}_p$, $\mathbf{K}_v$, $\mathbf{K}_f$, $\mathbf{K}_{fi}$ are square diagonal coefficient matrices of PD position controller and PI force controller. This set of regulators gives higher priority for the force control. **J** is for Jacobian matrix and KIN means forward kinematics of manipulator.

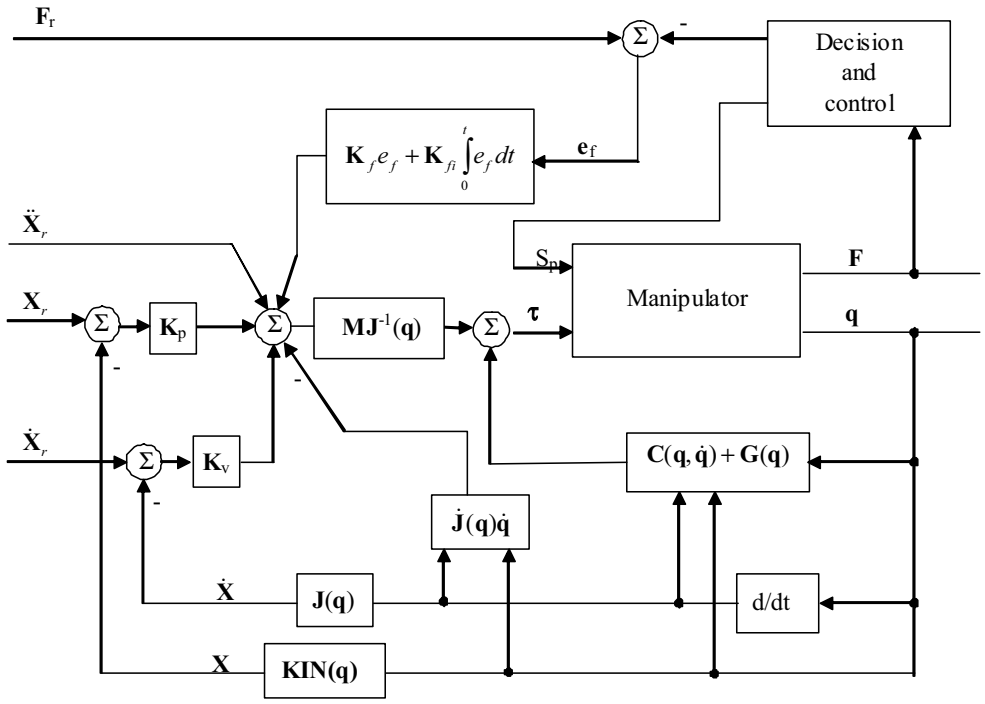

Figure 17. Block diagram of simultaneous position and force control

Block Manipulator includes all low level controllers: model of transmission system, force and stiffness generator and pressure controllers. The decision and control block monitors contact forces and swithces force control loop on and off. It also decreases stiffness of joints.
Some experiments are shown in Fig. 18. Manipulator follows the Cartesian trajectory in free space (see Fig. 18a) with zero contact force. In the next run an obstacle is placed in the working space of manipulator as shown in Fig. 1. When robot touches this obstacle the force control loop is activated. End-effector continues position trajectory in x direction while in y direction force rises to 30N and remains on this level (see Fig. 18c). In this experiment stiffness is constant through all the time.
To show the influence of stiffness of manipulator's joints on the transient phase of contact we repeated the same experiment with obstacle but we ordered control system to decrease stiffness when contact appears. The results are shown in Fig. 19, with highlighted region of plots where some improvements can be observed. In the circle one can see much smoother force trajectory almost without any shock. Pneumatic drives with their natural compliance behaves very well in contact actions even without the last improvement.

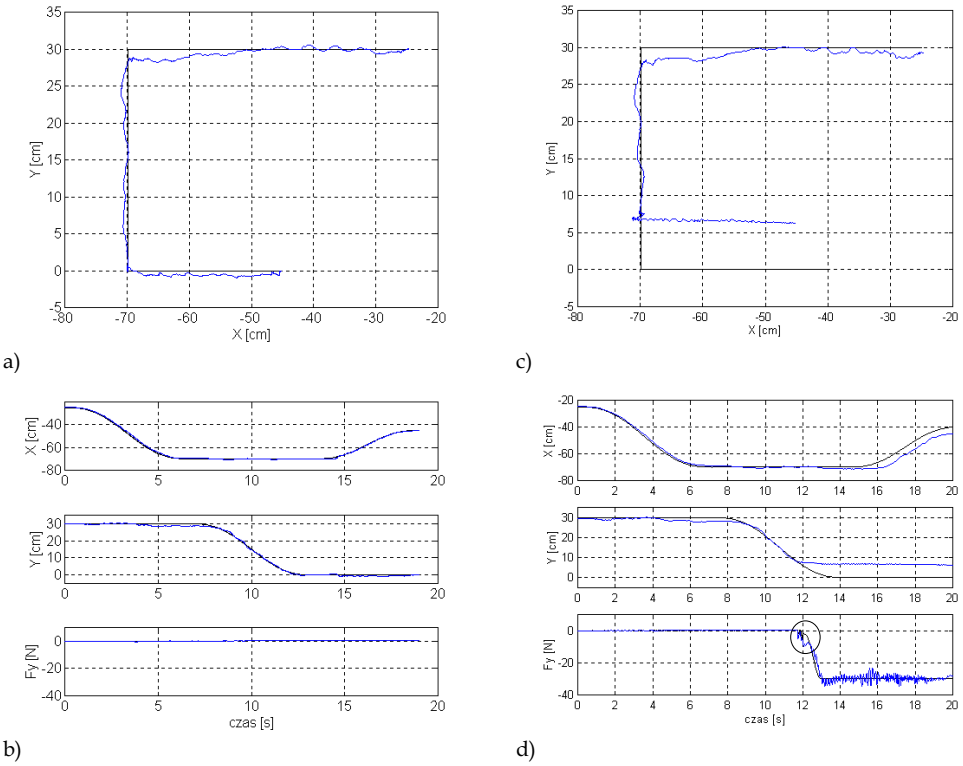

Figure 18. Position-force control of TM44 manipulator: a) Cartesian trajectory in the free space, b)position and force tracking – no contact, c) kartesian trajectory in the obstacle space, d)position and force tracking – contact with an obstacle

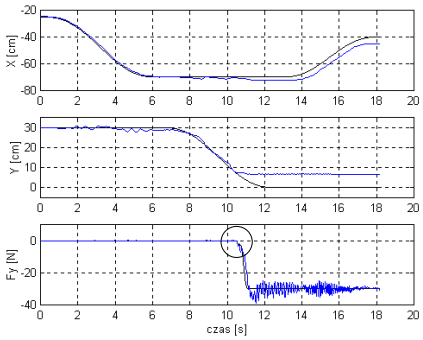

Figure 19. Position force control with stiffness regulation

5. Walking and climbing quadrupeds

The next application employing pneumatic driving system is the pair of low cost and easy to build walking and climbing robots that our students made as graduation project (Dąbrowski et al., 2001). Two levels of reduction of complexity of driving system and its influence on flexibility and mobility of robot will be shown here.
Two quadruped mechanisms mimicking the constitution of a turtle have been considered. Both of them have the same general structure schematically shown in Fig. 20. Each leg can rotate around vertical axis and has constant length. It gives the simplicity of the construction however required some modifications of the natural gait pattern.

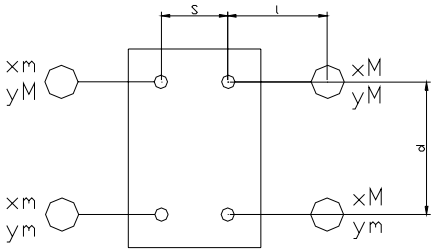

Figure 20. Geometrical structure of quadruped robot

First construction has four independently driven limbs moving in horizontal plane and additional vertical actuators for lifting, and vacuum cups on each leg. Therefore, each leg has 2 degrees of freedom and can be driven separately. Vacuum cups improved stability of static behaviour of robot and gives additional possibility of climbing. Walking strategy of this robot was generated based on mimicking turtle movement. With compliant pneumatic limbs robot can walk even when trajectory tracking is not ideal.
Second construction (see Fig. 1) is maximally reduced, with four coupled limbs driven by two actuators only. The limbs of this robot are also equipped with vacuum cups. Less components means lower weight and therefore robot can easily climb vertical walls. This underactuated robot requires coordinated lengthening of one side cylinder with shortening of another, correlated with switching of suction cups. This synchronization was obtained with only two 5/2 switching valves what is one more advantage of simple off-the-shelf pneumatic components.
The schemes of pneumatic connections in both robots are presented in Fig. 21. It is worth to compare the complexity of both solutions and their mobility. First robot is equipped with 16 electro-pneumatic 3/2 valves. Regulation of movements of main cylinders driving legs is reached by PWM modulation of valves while vertical actuators and ejectors work under static on/off regime. Legs can follow any position trajectories. The control algorithm has hierarchical structure containing task generator, gait pattern scheduler and valve control level. This robot can recognise five orders: forward and backward move, turn the right and left, and stop. Driving system of second robot is extremely reduced, in contrary. The possible tasks are reduced too, of course. This robot can move forward and backward, and stop on any flat surface with elevation angle in the range 0-90 deg. Further rearranging of a driving system and adding two 3/2 valves for vacuum cups can extent mobility of this robot (turn to the right and left functions) and can give possibility of walking on the ceiling. Such an experiment has been performed, too.

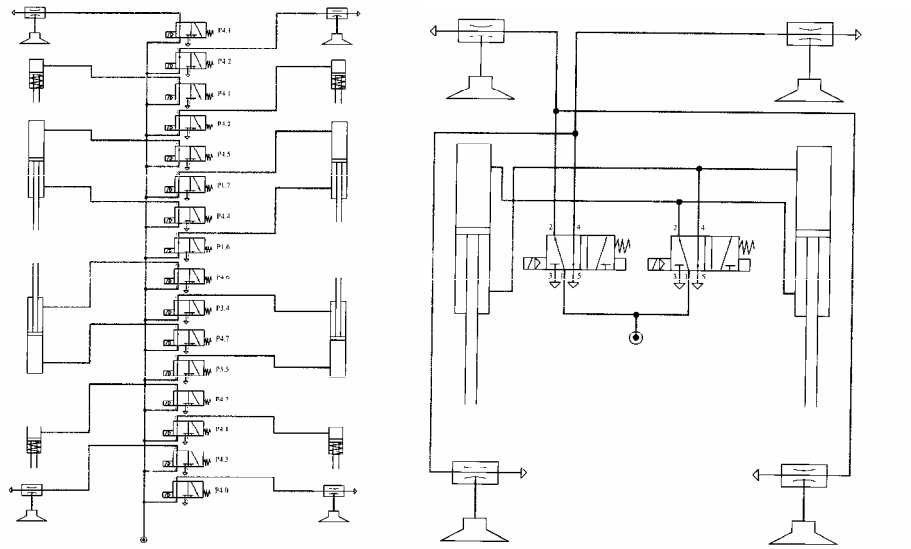

Figure 21. Pneumatic connections in walking robots: independently driven legs (left), coupled movement of legs (right)

6. Bellows driven, muscle steered caterpillar robot

This section presents the design of caterpillar-like robot Catty that utilizes only pneumatic actuators both for propulsion and steering. This approach gives our robot fully compliant behavior, which is advantageous in many cases. The aim of this research was to verify mobility of proposed design and applicability of caterpillar robot for inspection purposes. The prototype, shown in Fig. 22, comprise single segment and is able to perform 2-D motion on the smooth non-vertical surfaces. It can also bend the body almost 90deg in vertical plane, which gives opportunity for concave transitions.

Imitation of the nature is one of the most exploited methods used in design and control of robots. We also used this approach in some of the projects mentioned before and we proceeded the same way in this research. Caterpillar and inchworm locomotion drew attention of robot's designers due to its simplicity and effectiveness in very constrained spaces. These motion patters can usually be described using finite state models and thus make gait generation very easy (Chen et al., 2001). Our approach combines imitation of the nature with our experience with pneumatic actuators. We tried to model a multi-directional planar robot based directly on the original structure of caterpillar body and by taking advantage of natural elasticity of pneumatic bellows and muscles.

The idea of reciprocal movements in order to propel robot forward and backward is somehow similar to bridled bellows introduced by Aoki and Hirose in Slim Slime Robot (2002). However, in our design we use different technology – rubber bellows – specially designed for joint actuation in serpentine robots (see next section). These bellows have larger elasticity than any metal construction and, more important, large actuation strain (or simply speaking relative elongation). We also use muscles as steering actuators instead of motorized strings.

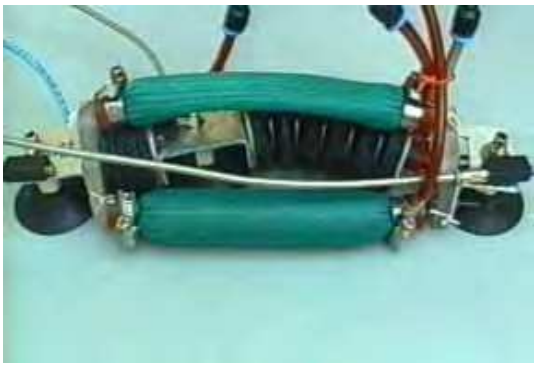

Figure 22. Robot Catty during turning procedure, muscle in first plane and bellows on the right are activated

During the simulation stage we developed simple gait patterns, which were experimentally verified on our test bed.We performed several tests to verify possibility of basic movements: straight locomotion, turning in spot and lifting up of the front part of the robot. All tests were performed on smooth and horizontal surface (Granosik & Kaczmarski, 2005).

7. The Integrated Joint Actuator for serpentine robot

Based on the discussion in section 3 we have chosen pneumatic bellows as the best-suited actuator for for serpentine robots. In accordance with that choice we designed the "Integrated Joint Actuator" (IJA) for serpentine robots. Fig. 23 shows a cross-section of the IJA. The design assumes that there is a 2-DOF universal joint in the center, connecting any two adjacent segments. An arrangement of four equally spaced bellows is used to actuate the two degrees of freedom of each joint. Each closed end of a bellows is rigidly fastened to the front or rear "firewall" of a segment. Compressed air can be pumped into the bellows or exhausted from the bellows via an appropriate hole in the firewall. The maximum bending angle in our IJA is up to 25° in each direction.

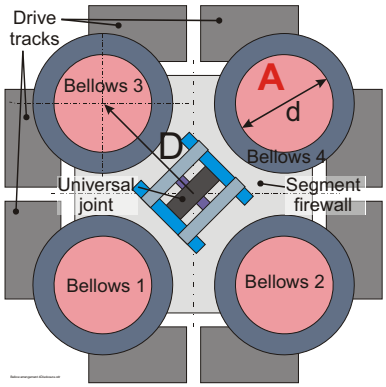

Figure 23. Cross-section of the integrated joint actuator

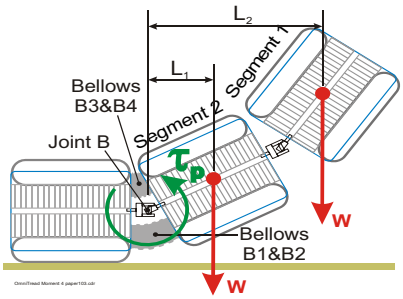

Figure 24. A typical task for a serpentine robot might involve the lifting of its first two segments to reach up to the top of a stair

In order to be able to traverse high obstacles, a serpentine robot should be able to lift as many segments as possible off the ground. As we will see below, though, the geometric shape of serpentine robots makes it extremely difficult to do so. To illustrate this problem, Fig. 24 shows the case of the OmniTread lifting its two lead segments, each of weight W. To accomplish this task, the IJA of Joint B inflates bellows B1 and B2 and exhausts bellows B3 and B4. This creates a lifting torque τ_p that must overcome the reactive moment from the weight of the two segments, $M_{react} = L_1W + L_2W$.

One must further keep in mind that in a fully symmetric serpentine robot, the vehicle has no "bottom" or "top." Rather, it can roll on any side and may even move on one of its four edges (as can be visualized by thinking of Fig. 23 rotated 45° clockwise or counter-clockwise). In such an extreme case, only one single bellows would be able to contribute to the lifting torque τ_p. In this case, the lever arm for producing this lifting torque has length D, as shown in Fig. 23.

For the worst case of the OmniTread laying on its edge, the lifting torque τ_p produced by a single pair of opposite bellows was given by Eq. (7).

$$\tau_p = DA(p_A - p_B) \tag{7}$$

During experiments we have measured the minimum value of the pressure difference $(p_A - p_B) = 4.34$ bar needed for generating a torque $\tau_p = 25$ Nm. This torque is sufficient to lift up the two lead- or tail-segments.

In the nominal case of Fig. 24 (OmniTread laying on a side, not an edge), not just one but two bellows-pairs provide the lifting torque, albeit at a reduced moment lever $D/\sqrt{2}$. The available lifting torque in that case is larger than in the case of the OmniTread laying on its edge and can be generated by an even smaller pressure difference. In this case two front segments can be lifted up by the pressure difference $(p_A - p_B) = 3.24$ bar generating a torque $\tau_p = 27$ Nm.

What we like the most in our IJA is the way it fits in so called *joint space* between two segments as shown in Fig. 25. Because of their inherent geometric characteristics, cylinders and McKibben muscles would have to be placed within a segment to actuate the joints (like in OmniPede design). In contrast, pneumatic bellows are an ideal solution, because they allow the integration of one or more large-diameter pneumatic actuators in the space of the joint, without requiring any space within a segment. Shape of a *joint space* varies as a function of joint angles. Because of these variations, the largest rigid component that can be mounted in joint space has to be limited in size to fit into the volume of "minimal space", that is, the space that's available where two segments are rotated toward each other (left side on the photo of OmniTread's joint, Fig. 25).

Figure 25. Joints of serpentine robots: OmniPede the predecessor of OmniTread with pneumatic cylinders (left), Integrated Joint Actuator in OmniTread (right)

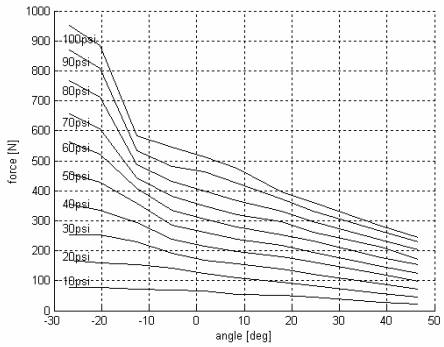

Figure 26. Force characteristics of the single bellows for angular actuation in IJA

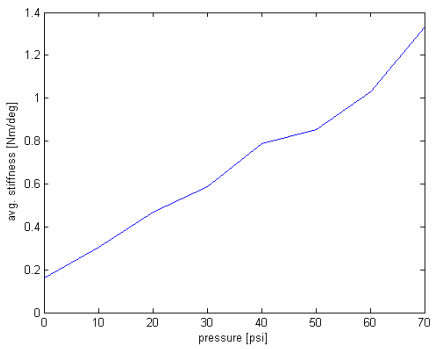

Figure 27. Average stiffness of the joint vs. pressure level in bellows

In practice, this means that joint space cannot be used for any rigid component, because adjacent segments almost touch when fully rotated toward each other. In contrast to rigid components, bellows have the very suitable property of taking up minimal space when deflated, and maximal space when inflated. They can thus be placed in joint space, without taking up any segment space.

On the special test bed, using the same components of IJA and equipped with force sensor and potentiometer we have obtain characteristics showing relation between force exerted to the segment of the robot and angular position of the joint, shown in Fig. 26.
On the same test bed we experimentally checked the relation between elasticity of a joint and the level of pressures in bellows. We measured forces necessary to move a joint in different directions of its freedom together with related angles. We repeated experiments for several levels of pressures in the range from 0 to 5 bar. The average value of stiffness was calculated as $S=Fr/\alpha$ where F – external force causing the angular displacement α, r – arm of the force F and plotted with reference to level of pressures in Fig. 27. As we could expect from spring-like nature of bellows relation is close to linear with standard deviation less then 10%. As bellows are identical and have the same spring coefficient they tend to create a stable, straight-line posture for the segments. This is the case regardless of whether all bellows are (equally) charged, exhausted, or closed.
In our paper (Granosik & Borenstein, 2005) we have proposed a control system for joints of OmniPede called "Proportional Position and Stiffness" (PPS) controller. The PPE system is designed to do what its name implies: it allows for the simultaneous and proportional control of position and stiffness of pneumatic actuators. The PPS controller is further optimized for use in mobile robots, where on-board compressed air is a valuable resource. To this end, the PPS employs a uniquely designed system of valves that assures that compressed air is consumed only during commanded changes of pressure or stiffness, but not while an actuator is held at a constant pressure and stiffness.
However, the PPS controller is based on an approximated model of cylinders and requires the real-time measurement of certain system parameters. For example, the polar moment of inertia of masses that are being moved by the joint must be known at all times, as well as the torque needed to move the joint. In complex environments where the serpentine robot may be laying on any side additional sensors would be needed to measure these parameters.
In the OmniTread these sensors were not implement. However, we were able to simplify the control system so that these sensors are not needed, while maintaining acceptable performance. We call it "*Simplified Proportional Position and Stiffness*" (SPPS) controller. The SPPS controller uses a PID position controller with a stiffness control subsystem, as shown in Fig. 28.

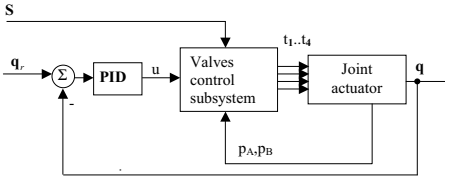

Figure 28. Block diagram of the Simplified Proportional Position and Stiffness (SPPS) system with zero air consumption at steady state

The task of the control system is to control the position of a joint, as well as its stiffness. The controlled parameters are the pressures p_A and p_B in the bellows-pair that actuates the joint. In order to control p_A and p_B, the PID controller generates the control signal u as input for the valve control subsystem. This subsystem realizes the stiffness control and air flow minimization by activating the four pneumatic valves according to the flow chart in Fig. 29. In every control cycle only one of the four valves is active, i.e. generates airflow to or from one of the bellows. Performance of OmniTread and its ancestor – OT4 – is presented in our paper (Granosik et al., 2007).

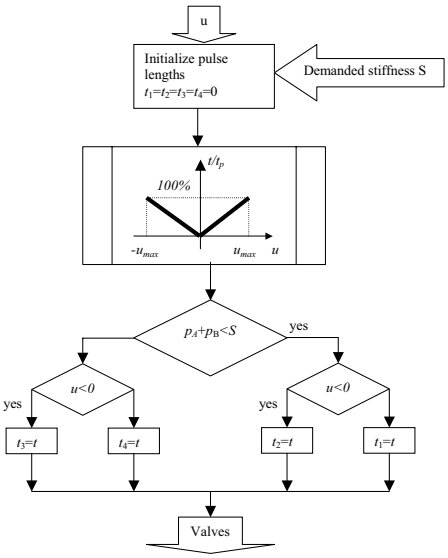

Figure 29. Flow chart for the valve control subsystem

8. Conclusion and future work

Pneumatic actuators originally limited to simple motion between two hard stops, are now becoming more and more popular, and substituting in many cases electric drives. Especially robots intended to contact with ground, obstacles, co-operating with other robots and humans require drives strong, compliant and safe. We have shown a few projects of quite different machines, all taking benefits from various pneumatic drives. But this chapter does not cover all important areas of possible applications for pneumatics.

Actuators with high power/weight ratio are needed in mechanical systems that support human motion in rehabilitation, welfare, and sports. Moreover, mechanical systems for entertainment requires various, smooth motions. Actuators applied to these systems also should have high power/weight ratio.

From biology we know that all animals, try to move in an energy efficient way. The important mechanisms available are muscles and tendons which make energy recuperation possible. For example, the Achilles tendon in a human leg can store up to one third of the motion's energy during running. The muscular system is capable of adapting stiffness characteristics in order to move in a wide range of different walking and running patterns and still exploit the passive behavior of the actuation system. This is why in the very first jumping robots thrust was generated by pneumatic actuator (Raibert, 1986). In this area we focus our investigations on the aspect of changing mechanical impedance of driving system and its influence on features of a jump (Jezierski & Granosik, 2007).

Pneumatic drives can be combined with electric motors like in Distributed Macro Mini (DM2) Actuation concept (Zinn et al., 2004) producing hight performance and low impedance human safe actuator.

We also plan to use pneumatic elements for suspension of just beeing designed serpentine robot Wheeeler (Pytasz & Granosik, 2007).

9. References

Aoki T., Ohno H., Hirose S. (2002). Design of Slim Slime Robot II (SSR-II) with Bridle Bellows, *Proc. IEEE/RSJ Int. Conf.on Intelligent Robots and System*, vol.1, pp. 835-840.

Berns K., Albiez J., Kepplin V., Hillenbrand C. (2001). Airbug - insect-like machine actuated by fluidic muscle, *4th Int. Conference on Climbing and Walking Robots CLAWAR*, pp. 237–244, Karlsruhe, 24-26 Sept. 2001

Bobrow J.E., McDonell B.W. (1998). Modeling, identification, and control of a pneumatically actuated, force controllable robot, *IEEE Trans. on Robotics and Automation* vol.14, pp. 732-741

Borenstein J., Granosik G. (2005). *Integrated, Proportionally Controlled, and Naturally Compliant Universal Joint Actuator with Controllable Stiffness.* U.S. patent #6,870,343. (Rights Assigned to the University of Michigan)

Chen I.-M., Yeo S. H., Gao Y., (2001) Locomotive Gait Generation for Inchworm-Like Robots Using Finite State Approach, *Robotica*, Vol. 19, No.5, pp. 535-542.

Collie A.A., Granosik G., Jezierski E., Zarychta D., Mianowski K. (1996). Light–weight and compact manipulator for hazardous environment, *Proc. of 6th Int. Symposium on Measurement and Control in Robotics*, pp. 304-308, Brussels 1996

Dąbrowski T., Feja K., Granosik G. (2001). Biologically inspired control strategy of a pneumatically driven walking robot, *Proc. Of the 4th Int. Conference on Climbing and Walking Robots CLAWAR 2001*, pp 687-694, Karlsruhe 2001

Feja K. (2006). Kinematics of selected manipulators with multi DOF joints. (in polish) *Postępy robotyki. Sterowanie percepcja i komunikacja. Red. K. Tchoń*. pp. 37-46, WKŁ Warszawa, ISBN: 83-206-1628-X

Festo AG & Co, *Catalogue of Fluidic Muscle MAS*, www.festo.com.

Fukuda T., Kurashige K., Arai F. (1999). Recent topics on robotic actuation technologies, *Proc. of 2nd Int. Conference on Climbing and Walking Robots*, pp. 3-15, Portsmouth, 1999

Glenn K. K. (2000). Accounting for Elastic Energy Storage in McKibben Artificial Muscle Actuators. *Transactions of the ASME. Journal of Dynamic Systems, Measurement, and Control,* Vol. 122, pp. 386-388

Granosik G. (2001). Modelling of a pneumatic drive and correction of its dynamics for robotic application, *Proc. of 7th IEEE Int. Conf. on Methods and Models in Automation and Robotics MMAR 2001*, vol. II, pp 755-760, Międzyzdroje 2001

Granosik G. (2001b). Position/force control of a pneumatically driven robot arm, (in polish). *Proc. of VII National Robotics Conference*, Nr 103, t.2, pp 313-322, Lądek-Zdrój 2001

Granosik G., Borenstein J. (2005). Integrated joint actuator for serpentine robots. *IEEE/ASME Transactions on Mechatronics*, Vol. 10, pp. 473-481

Granosik G., Borenstein J. and Hansen M.G. (2007). Serpentine Robots for Industrial Inspection and Surveillance, in *Industrial Robotics. Programming, Simulation and Applications, Edited by Low Kin Huat*, pp. 633-662, Published by the plV pro literatur Verlag, Germany, February 2007, ISBN 3-86611-286-6

Granosik G., Jezierski E. (1999). Application of a maximum stiffness rule for pneumatically driven legs of walking robot, *Proc. of 2nd Int. Conference on Climbing and Walking Robots*, pp 213-218, Portsmouth 1999

Granosik G., Kaczmarski M. (2005). Bellows driven, muscle steered caterpillar robot, *Proc. of 8th Int. Conf. on Climbing and Walking Robots and the Support Technologies for Mobile Machines CLAWAR 2005*, pp. 743-750, London, UK, September 12-15, 2005.

Hirai S., Masui T., Kawamura S. (2002). Prototyping pneumatic group actuators composed of multiple single-motion elastic tubes, *Proc. of Journal of Robotic Society of Japan*, vol. 20, no 3, pp. 77-84, 2002

Huber J. E., Fleck N. A. and Ashby M.F. (1997). The selection of mechanical actuators based on performance indices, *Proc. of the Royal Society of London. Series A*. 453, pp. 2185-2205, UK1997

Jezierski E. (2006). *Robot Dynamics*, (in polish), WNT, Poland, ISBN 83-204-3128-X

Jezierski E., Granosik G., (2007). Modelling and Control of Jumping Robot with Pneumatic Drive, *Accepted to the IEEE MMAR Conference 2007*.

Knight R., Nehmzow U. (2002). Walking robots – a survey and a research proposal, *Technical report CSM-375 Department of Computer Science* University of Essex, UK 2002

Magnussen B., Fatikow S., Rembold, U. (1995). Actuation in microsystems: problem field overview and practical example of the piezoelectric robot for handling of microobjects. *Proc. INRIA/IEEE Symp. on Emerging Technologies and Factory Automation*, Vol. 3 pp. 21-27, 10-13 Oct.

Mattiazzo G., Mauro S., Raparelli T., Velardocchia M. (2002). Control of a Six-Axis Pneumatic Robot. *Journal of Robotic Systems* 19(8), 363–378

McMaster-Carr Supply Company, online catalogue: www.mcmaster.com

Morecki A. (2001). Polish artificial pneumatic muscle – design problems, *4th Int. Conference on Climbing and Walking Robots CLAWAR*, pp. 215-222, Karlsruhe.

Olszewski M. (1998). Position control of pneumatic drive, (in polish) *Pomiary Automatyka Robotyka*, nr 10, pp. 10-14 and 42-43, Poland

Pytasz M., Granosik G. (2007). Modeling and control of Wheeeler the hyper mobile robot, *Accepted to the IEEE MMAR Conference 2007*

Raibert M.H. (1986). *Legged robots that balance*, The MIT Press, 1986.

Robinson D.W. (2000). Design and analysis of series elasticity in closed-loop actuator force control, *PhD thesis, Massachusetts Institute of Technology* 2000.

Schultz S., Pylatiuk C., Bretthauer G. (2001). Walking machine with compliant joints, *4th Int. Conference on Climbing and Walking Robots CLAWAR*, pp. 231-236, Karlsruhe.

Shadow Robot Company, *Air Muscles*, www.shadow.org.uk

Shimizu T., Hayakawa Y., Kawamura S. (1995). Development of hexahedron rubber actuator, *Proc. IEEE Int. Conf. on Robotics and Automation*, pp. 2619-2624, Nagoya.

Sun L., Sun P., Luo Y., Zhang Y., Gong Z. (2001). Micro in-pipe robots with PZT actuator, *4th Int. Conf. on Climbing and Walking Robots CLAWAR*, pp. 539-546, Karlsruhe.

Suzomori K., Maeda T., Watanabe H., Hisada T. (1997). Fiberless flexible microactuator designed by finite-element method, *IEEE Trans. on Mechatronics*, Vol. 2, No. 4, Dec.1997

Tsagarakis N., Caldwell D.G. (2000). Improved Modelling and Assesment of pneumatic Muscle Actuators. *Proc. of IEEE Int. Conf. on Robotics and Automation*, pp. 3641-3646, San Francisco, USA

Van Ham R.R., Daerden F., Verrelst B., Lefeber D., Vandenhoudt J. (2002). Control of pneumatic artificial muscles with enhanced speed up circuitry, *5th Int. Conference on Climbing and Walking Robots CLAWAR*, pp. 195-202, Paris, 25-27 Sept. 2002

Verrelst B., Daerden F., Lefaber D., Van Ham R., Fabri T. (2000). Introducing pleated pneumatic artificial muscles for the actuation of legged robots: a one-dimensional set-up, *Proc. of 3rd Int. Conf. on Climbing and Walking Robots*, Madrid, 2-4 Oct.2000

Zinn M., Khatib O., Roth B., Salisbury J.K. (2004). Playing it safe [human-friendly robots]. *IEEE Robotics & Automation Magazine,* Vol. 11, Issue 2, pp. 12-21

Bioinspiration and Robotics Walking and Climbing Robots

Edited by Maki K. Habib

ISBN 978-3-902613-15-8
Hard cover, 544 pages
Publisher I-Tech Education and Publishing
Published online 01, September, 2007
Published in print edition September, 2007

Nature has always been a source of inspiration and ideas for the robotics community. New solutions and technologies are required and hence this book is coming out to address and deal with the main challenges facing walking and climbing robots, and contributes with innovative solutions, designs, technologies and techniques. This book reports on the state of the art research and development findings and results. The content of the book has been structured into 5 technical research sections with total of 30 chapters written by well recognized researchers worldwide.

How to reference

In order to correctly reference this scholarly work, feel free to copy and paste the following:

Grzegorz Granosik (2007). Pneumatic Actuators for Climbing, Walking and Serpentine Robots, Bioinspiration and Robotics Walking and Climbing Robots, Maki K. Habib (Ed.), ISBN: 978-3-902613-15-8, InTech, Available from: http://www.intechopen.com/books/bioinspiration_and_robotics_walking_and_climbing_robots/pneumatic_actuators_for_climbing__walking_and_serpentine_robots

INTECH
open science | open minds

InTech Europe
University Campus STeP Ri
Slavka Krautzeka 83/A
51000 Rijeka, Croatia
Phone: +385 (51) 770 447
Fax: +385 (51) 686 166
www.intechopen.com

InTech China
Unit 405, Office Block, Hotel Equatorial Shanghai
No.65, Yan An Road (West), Shanghai, 200040, China
中国上海市延安西路65号上海国际贵都大饭店办公楼405单元
Phone: +86-21-62489820
Fax: +86-21-62489821